High aspect ratio microstructuring of copper surfaces by means of ultrashort pulse laser ablation

Author(s):
Büttner, Henning; Hajri, Melik; Roth, Raoul; Wegener, Konrad

Publication date:
2018

Permanent link:
https://doi.org/10.3929/ethz-b-000311975

Originally published in:
Procedia CIRP 68, https://doi.org/10.1016/j.procir.2017.12.045

Available online at www.sciencedirect.com

ScienceDirect

Procedia CIRP 68 (2018) 190 – 195

www.elsevier.com/locate/procedia

19th CIRP Conference on Electro Physical and Chemical Machining, 23-27 April 2018, Bilbao, Spain

High aspect ratio microstructuring of copper surfaces by means of ultrashort pulse laser ablation

Büttner, H.[a]*, Hajri, M.[a], Roth, R.[a], Wegener, K.[a]

[a] *Institute of Machine Tools and Manufacturing, ETH Zürich, Leonhardstrasse 21, 8092 Zürich, Switzerland*

* H. Büttner. Tel.: +41 44 632 54 84; fax: +41 44 632 11 25. *E-mail address:* buettner@inspire.ethz.ch

Abstract

Laser beam machining (LBM) is capable of almost force-free 2D and 3D machining of any kind of material without tool wear. This process is defined by many parameters, such as pulse energy, frequency, scanning velocity and number of scanning repetitions. Modern laser machines provide high energy at shorter pulse durations and have more precise positioning systems than machines of the past. These can easily fulfil today's continuous changing product requirements. For an overall understanding, an extensive amount of experimentation is required to display the interaction laws and dependencies between process parameters, as well as the resulting shapes and quality of the machined surface. By using an ultrashort pulse (USP) laser, a wide range of customer oriented applications in micrometer scale can be addressed, which leads to precise ablation with minimal thermal damage. This paper provides knowledge on the machining of copper micro features with high aspect ratio and a 532 nm wavelength laser beam. Aspect ratios up to 17 and slot widths smaller than 20 µm were performed with a beam radius ω_0 smaller than 5 µm and pulse duration smaller than 12 ps. For desired slot geometries, necessary process parameters were developed and their physical limits are shown and discussed. The limits of minimum structure size have been analysed by observing the remaining material between slots at decreasing distances. Material debris deposits on the non-machined surface, as well as chemical changes of copper, were analysed using scanning electron microscope (SEM) and energy dispersive X-ray spectroscopy (EDX). Special attention was given to the taper angle, which arises due to the Gaussian distribution of energy in the laser beam.

Peer-review under responsibility of the scientific committee of the 19th CIRP Conference on Electro Physical and Chemical Machining

Keywords: micro machining; cold laser ablation; high aspect ratio

1. Introduction

Due to the constant development and improvement in the field of laser machining, precise structures in the micrometer scale can be machined. The ability to machine microstructures is desirable for many applications ranging from miniaturization to functionalization of large surfaces. Therefore a premise is the capability to reliably machine simple structures as slots. To this purpose micromachining of copper surfaces by means of ultrashort pulse (USP) lasers will be discussed in this paper. To gain further knowledge about the physical interaction of light with pure copper, a parametric analysis was carried out. Slots with varying width and depth were machined with the aim to maximize the resulting aspect ratio while minimizing the thermal damage. In this paper is shown that aspect ratios up to 17 are feasible to produce. However, the coupling between the resulting width and depth of slots limits the feasibility of micro machining. Taper angle formation, and thus the reduction of fluence, limits the attainable geometries. It is shown, that machining settings must be chosen interdependently. Due to saturation of depth, a continuous increase of pulse energy leads to thermal damage. Augmenting the number of repetitions, however, results in inefficient machining durations and negative taper angles,

Peer-review under responsibility of the scientific committee of the 19th CIRP Conference on Electro Physical and Chemical Machining
doi:10.1016/j.procir.2017.12.045

which is not beneficial for technical applications. To machine flawless micro structures the right process parameter combinations have to be found.

Nomenclature

d	depth	[µm]
d_{entry}	diameter at entrance	[µm]
d_{exit}	diameter at exit	[µm]
EDX	energy dispersive X-ray spectroscopy	
E_p	pulse energy	[J]
F	fluence	[J/cm^2]
f	frequency	[kHz]
F_{Peak}	peak fluence	[J/cm^2]
F_{th}	threshold fluence	[J/cm^2]
l	flank length	[µm]
LBM	laser beam machining	
MRR	material removal rate	
N	number of repetitions	
r	ablation radius, where F_{th} is reached	[µm]
R^2	coefficient of determination	
SEM	scanning electron microscopy	
t	thickness	[µm]
USP	ultra short pulse	
v_{scan}	scanning velocity	[mm/s]
w	entry width of slot	[µm]
α	absorption coefficient	[1/cm^2]
θ	taper angle	[°]
$\omega_{(z)}$	radius of laser beam at position z	[µm]
ω_0	radius at laser beam focus	[µm]

2. Physical background

2.1. Cold ablation for precision machining

The entire process depends highly on processing conditions, such as laser beam characteristics, environmental influences, properties of the material to be machined and initial surface topography. Losses by reflection and scattering whilst heat diffuses into the bulk matter changes the material removal behavior. For precise micro machining using laser ablation, the pulse duration plays a dominant role over the process of material removal.

Laser beam machining can be classified as cold or hot ablation. Regarding to A. Miotello and R. Kelly [8] by using USP laser for the cold ablation, two types of thermal process for material removal can be considered. In the first type normal vaporization on the impact zone happens at any pulse length. The subsequent flux of atoms per square centimeter and seconds is defined by the Hertz-Knudsen equation. In the second type of thermal process the laser fluence must be sufficiently high and the pulse length sufficiently short. In those conditions homogeneous bubble nucleation occurs and the impinged matter transits from superheated liquid to a mixture of vapor and equilibrium liquid droplets. Thus, type two can be determined either as phase explosion or explosive boiling. According to Martynyuk [7], in explosive boiling, the superheated melt undergoes an explosive liquid-vapor phase transition into a stable two-phase state. Lutey [6] excludes normal boiling of matter within pulse duration up to 500 ns. At longer pulse durations hot ablation initiates, where material removal happens due to sublimation and evaporation. To achieve negligible thermal damage and burr free surfaces, cold ablation should be used. This can be provided by ultrashort pulse laser machines, which can generate pulse durations shorter than 10 picoseconds. Neuenschwander et al. [9] observed an increase of workpiece quality by working in the sub picosecond field. According to Boerner et al. in [1] the electrons start to relax and conduct energy to their neighbor crystal lattice structure when pulses exceed the duration of 10 ps in copper material.

2.2. Ablation theory

Micro laser beam machining is an ablation process in which a beam of high intensity impinges onto a workpiece. The spot, where energy is sufficiently high to vaporize the substrate, causes material removal. The energy needed for removal is declared as the material dependent threshold fluence F_{th}, which must be exceeded by the fluence F provided by the laser beam. By setting up an excessive fluence $F >> F_{th}$, thermal damages happen on the impact zone. Those can appear as melting pools and burrs. However, a massive material removal is feasible, which can be beneficial in roughing operations.

The fluence F is defined as energy per area and is calculated as Eq. (1):

$$F(r,z) = \frac{2E_p}{\pi\omega_{(z)}^2} e^{-2\frac{r^2}{\omega(z)^2}} \quad (1)$$

with E_p the pulse energy, $\omega_{(z)}$ the radius of the laser beam at position z in the propagation direction of the beam and r the radius where F_{th} is reached. The term $2E_p/\pi\omega_{(z)}^2$ indicates the peak fluence. Along the propagation direction, the beam converges to a waist onto the beam focus and from there it spreads diverging.

According to Fig. 1 (a) the ablation radius r, where efficient material removal is possible, is given by the threshold fluence F_{th} and can therefore vary in function of the peak fluence F_{Peak}. The higher the peak fluence F_{Peak} is, the higher is the ablation radius r. According to Jaeggi et al. [5], the spatial Gaussian intensity distribution of the beam leads to the characteristic ablation profile introduced by one pulse in a shape of a parabolic function with a depth d, see Fig. 1 (b). Hashida et al. [4] interrelated the limitation of ablation depth d [cm] of the first pulse to the absorption coefficient α [1/cm^2] and threshold fluence of the material. Based on this, a logarithmic dependence of ablation depth can be found as Eq. (2):

$$d = \frac{1}{\alpha}\ln\left(\frac{F}{F_{th}}\right) \quad (2)$$

To increase the depth, the fluence can be adjusted, which will cause thermal damage in some conditions. As an alternative, the amount of pulses can be increased in order to penetrate the pre-machined surface multiple times. The depth

of the impact zone converges after several pulses to a lower limit.

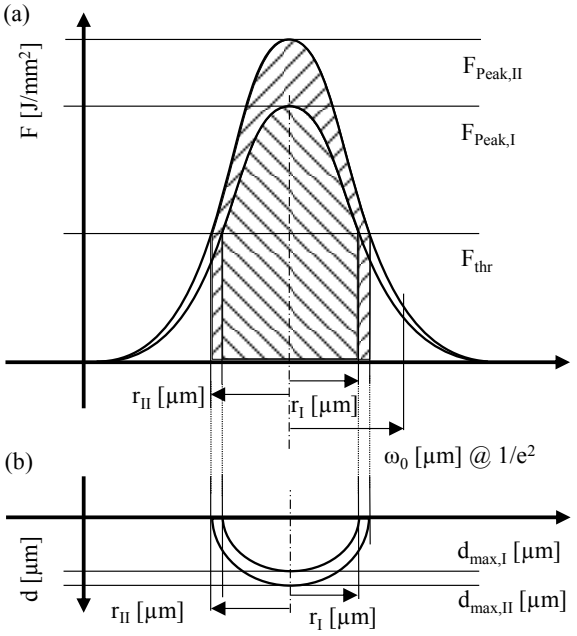

Fig. 1. (a) Gaussian distribution of laser beam; (b) shape of ablation crater.

In Fig. 2 (a) a crater can be seen after the laser beam was directed perpendicular to the surface, which maximizes the effective absorbed surface energy density. By setting up a higher number of repetitions N according to Fig. 2 (b) – (d) the ablation depth increases, however saturation becomes clearly pronounced. The sequent pulses interact with an inclined surface, whereas in Fig. 2 (a) the first pulse interacts with a normal incidence on the surface. Due to the inclination of the flank, the beam illuminates a larger area, thus the fluence decreases and the material removal rate drops. In addition to the downgrade of the fluence, the losses by reflection and scattering change for the worse. However, as shown in Fig. 2 (e) the material removal of a single pulse decreases with the number of pulses.

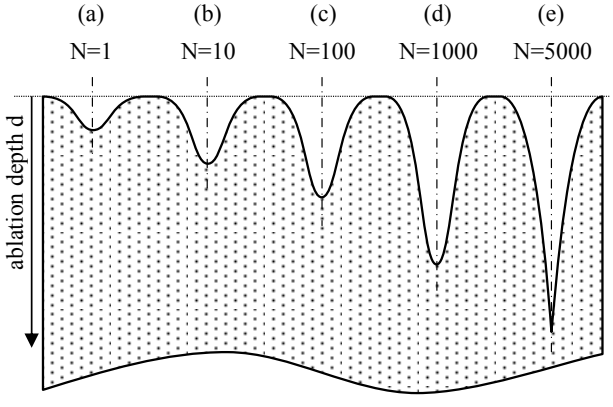

Fig. 2. schematic representation of ablation depth and crater shape in dependence of number of repetitions N.

Yeo et al. suggested in [12], that by increasing the aspect ratio, multiple reflections from the crater walls at shallow angles of incidence channel the optical energy to the center of the crater. Summarizing, the reduction of fluence and the losses from reflection in primal pulses limit the achievable crater depth.

2.3. Taper angle measurement

The appearance of the taper angle reduces the quality of a micro structured surface, hence the inclination of machined flanks differ from a desired shape.

For the evaluation of the taper angle only the middle 80 % of the flank length l are taken into account to exclude edge effects. Thawari et al. [3], Pfeifer et al. [10] and Dubey and Yadava [2] described the taper angle θ in laser drilling as Eq. (3) :

$$\theta = \tan^{-1} \frac{d_{entry} - d_{exit}}{2t} \tag{3}$$

where d_{entry} is the entrance, d_{exit} the outlet diameter and t the thickness of the material to be machined. In fact, in this present research no material through cut happens, the taper angle θ must be calculated as Eq. (4):

$$\theta = \cos^{-1} \frac{0.8d}{l} \tag{4}$$

For this calculation method a linear interpolation of the middle 80% of the depth (ignoring the top and bottom 10% depth) is used to evaluate the length l. The taper angle can be calculated with the cosines of the ratio between 80% of the depth d and the length l.

3. Preparation

3.1. Machine setup

For the investigations a DUETTO ultrashort pulse laser machine from TIME-BANDWIDTH PRODUCTS was used, which generates pulse durations as low as 12 ps. The device provides an average laser power of 15 W at 1064 nm and pulse energies up to 200 µJ with frequencies up to 50 kHz. The wavelengths can be set to 355 nm, 532 nm and 1064 nm. The laser beam wavelength was set to 532 nm because of the considerably lower reflection-absorption-ratio in copper machining with lower wavelength. For feed direction, independent machining circular polarized light was used, which can be achieved by applying a λ/4-polarization filter.

3.2. Analyzing methods

Microscopy cannot gather sufficient information from depths with high aspect ratios. To visualize the machined slot profile, a cross section of all specimens was made by electric discharge wire cutting. This cutting process introduces mechanical and thermal stresses, therefore the cross sections were ground and polished. Super-finishing was performed by etching. The prepared slot profiles are recorded with an ALICONA INFINITEFOCUS Microscope. To ensure repeatable measurements, a MATLAB image recognition script was

programmed to investigate quality attributes, such as width, depth and material removal rate, as well as the taper angle.

4. Experimentation

4.1. Slot-experimentation

In precise micro machining using laser ablation, the geometric accuracy of the structure is a matter of substantial interest. The depth of ablation can solely be calculated with the two-temperature-model, which is highly dependent on material properties and laser process parameters. Hence, an analytical prediction of contour divergence cannot be performed without an extensive amount of experimentation. Engelhardt et al. [11] described the material removal per pulse correlated to the fluence used. By increasing the fluence, the material removal leads to saturation. But before saturation is reached, thermal damage may be limiting for the process. To reach higher material removal, the repetition of scanning passes is increased. Its effect is limited by the formation of taper angle and defocusing, thus lowering of local fluence. Beside the laser process parameters, also the properties of the scanning system play a role in material removal. In the performed experimentation, slots with a length of 5 mm are machined for each setup. The maximum feasible aspect ratio in the µm-range is investigated. The applied parameters for the investigations are given in Table 1.

Table 1. process parameters for slot-experimentation.

Parameter	Value	Unit
pulse energy E_p	1.1 … 30.7	µJ
frequency f	50	kHz
scanning velocity v_{scan}	50	mm/s
repetitions N	10 … 5000	
laser beam focus radius ω_0	< 5	µm
wavelength	532	nm
pulse duration	12	ps

The formation of the taper angle limits the attainable depth. In Diagram 1 it is shown that a maximum depth d = 430 µm is achieved with N = 5000, however 81 % of the depth was already reached after N = 1000. By keeping N = 5000, 70% of the depth can be reached with 37 % pulse energy of E_p = 30.7 µJ.

Diagram 1. Depth of slot vs. repetitions of machining passes.

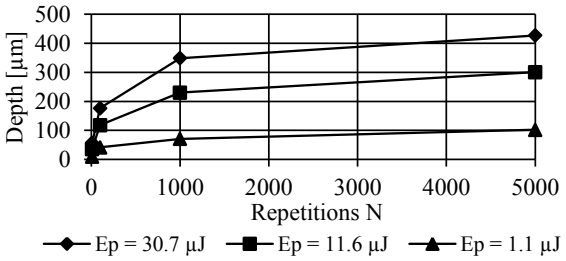

Diagram 2 visualizes that a slot width larger than the laser beam focus radius ω_0 can be machined. The width w can be maximized by increasing the number of repetitions N or the pulse energy E_p and reached up to w = 27 µm. In the first 1000 repetitions, 69 % of the final width was already reached by using E_p = 30.7 µJ. With 36 % of the final applied pulse energy E_p, 77 % of the final width was already generated.

Diagram 2. Width of slot vs. repetitions of machining passes.

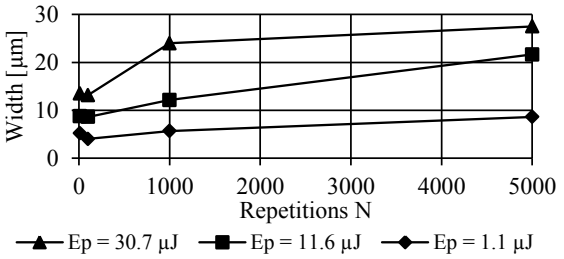

Diagram 1 and Diagram 2 show, that a given depth or width can be machined with different combinations of pulse energy E_p and repetitions N. In a physical point of view, this assumption misrepresents the power of those parameters. On the one hand, the machining time leads to an inadmissible duration with numerous repetitions. To reach slots with high quality and extreme aspect ratios, a trade-off must be made with the machining time, respectively the material removal rate (MRR). Due to the saturation behaviour of the depth the MRR drops drastically by raising up the number of passes. 80% of total material removal is achieved during the first 100 repetitions when using maximal pulse energy. Over the first 1000 repetitions 90% of the material is removed. An increase of 4000 repetitions merely leads to an additional 10% material removal after a machining duration that is four times longer. On the other hand, higher pulse energy may damage a target slot shape.

Diagram 3. Depth of slots vs. width of slots.

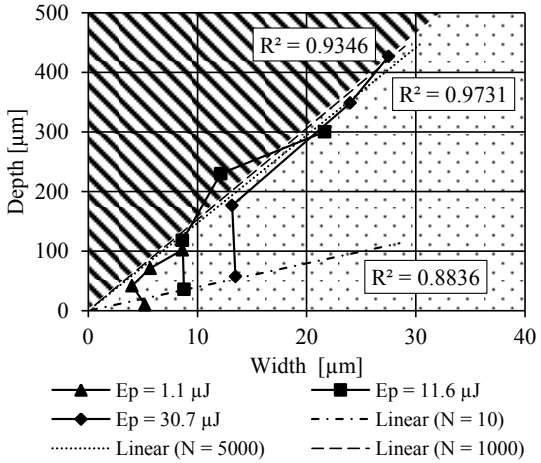

A correlation between the width w and depth d of a slot can be found, according to Diagram 3. To increase the depth the number of repetitions must be increased, however, saturation was observed. The depth cannot be set up independent from the width, because the depth saturates by an increase of the number of repetitions. Therefore, shifting the limit must be performed by increasing the pulse energy E_p, but this leads to further enlargement of the width. The fitted lines of N = 10, N = 1000 and N = 5000 predict the formation of the slot dimensions. The lines intersect in the origin, where

the dimensions are zero. The hatched region is out of the possible machining range. High aspect ratios up to 17 are achieved. Before saturation of the depth growth, the depth develops faster than the width. Yet the width continues to grow by further repetitions, even when the depth growth is saturated. This effect leads to a reduction of the aspect ratio.

It is found that the taper angle is strongly dependent on the number of repetitions, see Diagram 4. Over the initializing repetitions, the pulse energy plays an influential role. The effect of pulse energy decreases after an increase of repetitions. It was observed that above a certain number of repetitions the taper angle falls below zero, which might be explained by multiple reflection effects. Multiple rays of reflected light are held captive on the bottom of the slot if the aspect ratio exceeds 1:13 for E_p = 2.8 µJ and respectively 1:17 for E_p = 30.7 µJ. The material removal continues at such aspect ratios due to less scatter losses at multiple reflections, which leads to a greater width at the bottom compared to the width at the entry of the slot, see Fig. 3 (b).

Diagram 4. Taper angle vs. repetitions of machining passes.

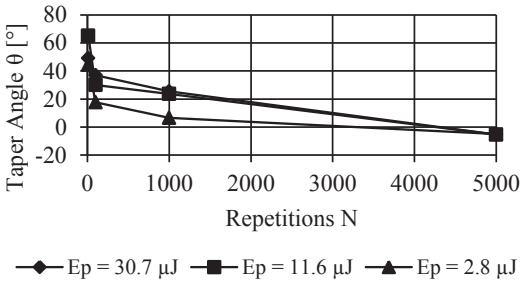

Final slot geometries of high aspect ratio and steep flanks are shown in Fig. 3 (a) and (b). The slot in Fig. 3 (a) was machined by using a pulse energy E_p = 30.7 µJ and a number of repetitions N = 1000, whereas the slot in Fig. 3 (b) was machined with E_p = 30.7 µJ and N = 5000, however ramification, which is defined as deviations from the theoretical straight path, are clearly pronounced with rising repetitions.

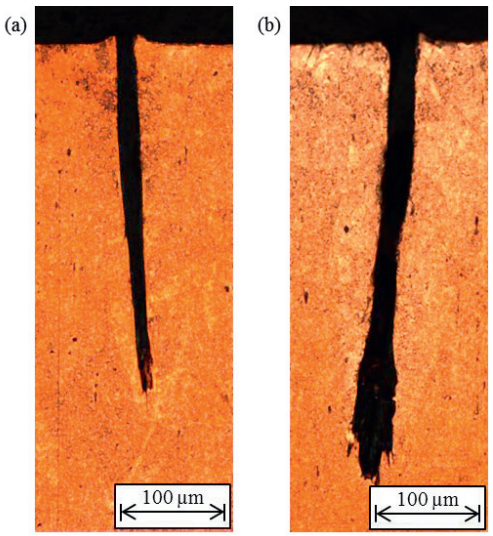

Fig. 3. (a) slot with technical relevance; (b) slot with ramification.

In Fig. 3 (a) the depth is 340 µm and the width is 21 µm and at a higher amount of repetitions, in Fig. 3 (b) the depth increases to 441 µm and the width to 29 µm. Due to steep flanks with a taper angle of θ = 4.8° Fig. 3 (a) delivers a satisfying result, however the taper angle decreases down to θ = -8° in Fig. 3 (b).

4.2. Thermal damage

For single slot machining, many process parameter combinations are feasible to fulfill necessary geometrical requirements. If a slot is machined in bulk material, thermal effects to the surrounding material can be neglected if high thermal conductivity is guaranteed. Multiple slot-experimentation leads to the detection of thermal influence respectively damage of surrounding material as a consequence of heat accumulation. Thus, the remaining material can bend and melt. This is why multiple slots were machined and aligned together with a defined pitch. The used parameters are shown in Table 2, which generate slots with equal widths and equal depths.

Table 2. Parameter setup for multi-slot with constant pitch.

Figure	Ep [µJ]	N	width slot [µm]	depth slot [µm]	pitch bar [µm]	width bar [µm]
3 (a)	30.7	42	10	100	20	10
3 (b)	7.2	100				
3 (c)	2.8	1000				
3 (d)	1.1	5000				

With high pulse energy, thermal damage shown in Fig. 4 (a) occurs. The remaining bars are supposed to retain a width of 10 µm in a theoretical point of view, but thermal damage removes the surrounding material. Due to heat accumulation the copper material starts to bend in Fig. 4 (b) without any further ablation of remaining bars. In Fig. 4 (c) a better result is achieved. The bars present a normal orientation related to the surface. With an extreme number of repetitions in Fig. 4 (d) ramification is highly developed due to multiple reflections on the bottom of the slots.

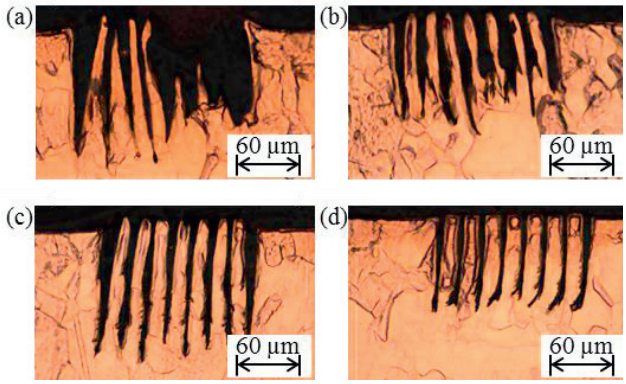

Fig. 4. Thermal damage at multi-slot generation, shown in a cut image; (a) destruction of slots due excessive pulse energy; (b) bending of remaining material due to head accumulation; (c) satisfying result by setting up a trade-off between pulse energy and repetitions; (d) ramification introduced by an excessive number of repetitions.

5. SEM & EDX

Chemical modifications of copper bulk material due to laser machining were investigated using energy dispersive X-ray spectroscopy (EDX). Three representative machining settings are compared in Diagram 5.

Diagram 5. EDX-analysis of machined copper specimen normalized to the copper peak at 0.9 keV; magnified to oxygen regimen (C = Carbon, O = oxygen, Cu = Copper).

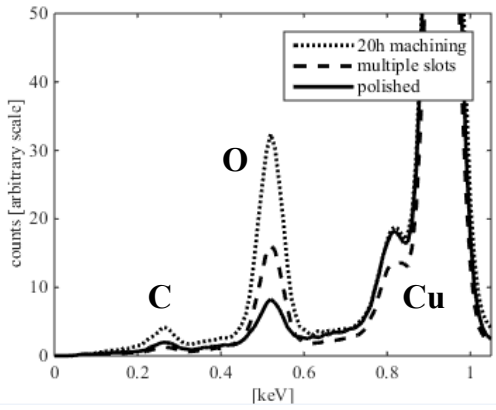

The polished copper specimen acts as benchmark. To show differences between two settings, extreme machining durations are compared. An excessive amount of repetitions, leading to a machining time of over 20 hours, and an optimized amount of repetitions are used to show the influence of machining time. EDX analysis shows a constant material composition, but the amount of each element changes. By increasing the machining time a proliferation of oxygen was found.

In Fig. 5 two slots and a remaining bar is shown from the top view by using scanning electron microscope (SEM). On the pre-machined surface, debris of removed material was impinged and deposited. Debris impingement was found in all experiments, hence a correlation with machining settings cannot be established.

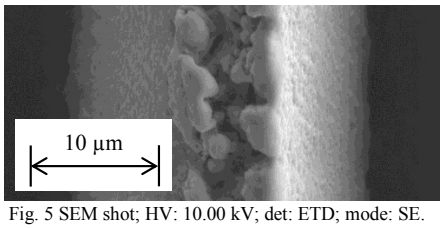

Fig. 5 SEM shot; HV: 10.00 kV; det: ETD; mode: SE.

6. Conclusion

The machining of flawless micro structures using laser beam ablation is highly dependent on the setup of process parameters. It was found that resulting depth is coupled with width and vice versa. For a given slot geometry, different parameter combinations are possible:

- High pulse energy primarily develops the depth, but a widening of slots is foreseeable.
- Slot shape can be defined beside the pulse energy by the number of repetitions. An excessive number leads to inefficient machining durations and ramification at the slot bottom due to multiple light reflections.
- To avoid thermal damage, a trade-off between pulse energy and number of repetitions must be defined.

The challenges of machining microstructures by using laser beam ablation are discussed. The limits of slot geometries and deformation effects are shown. Reliable machine setting for machining single slot as well as multiple slots with a defined pitch to each other is presented. However further research is necessary to machine discretionary micro structures, such as pillars and cavities.

References

[1] Boerner, P., Zandonadi, G., Eberle, G., Wegener, K., 2015, Experimental and modelling investigations into the laser ablation with picosecond pulses at second harmonics, Conference on Laser-Based Micro- and Nanoprocessing IX, San Francisco, CA, USA, February 10-12, 2015, 9351/:935104.

[2] Dubey, A. K., Yadava, V., 2008, Robust parameter design and multi-objective optimization of laser beam cutting for aluminium alloy sheet, The International Journal of Advanced Manufacturing Technology, 38/3:268-77.

[3] G. Thawari , J. K. S. S., G. Sundararajan, S.V. Joshi, 2005, Influence of process parameters during pulsed Nd:YAG laser cutting of nickel-base superalloys.

[4] Hashida, M., Semerok, A. F., Gobert, O., Petite, G., Izawa, Y., Wagner, J. F., 2002, Ablation threshold dependence on pulse duration for copper, Applied Surface Science, 197/:862-7.

[5] Jaeggi, B., Neuenschwander, B., Schmid, M., Muralt, M., Zuercher, J., Hunziker, U., 2011, Influence of the Pulse Duration in the ps-Regime on the Ablation Efficiency of Metals, Physics Procedia, 12/:164-71.

[6] Lutey, A. H. A., 2013, An improved model for nanosecond pulsed laser ablation of metals, Journal of Applied Physics, 114/8:083108.

[7] Martynyuk, M. M., 1977, Phase explosion of a metastable fluid, Combustion, Explosion and Shock Waves, 13/2:178-91.

[8] Miotello, A., Kelly, R., 1995, Critical assessment of thermal models for laser sputtering at high fluences, Applied Physics Letters, 67/24:3535-7.

[9] Neuenschwander, B., Jaeggi, B., Schmid, M., Rouffiange, V., Martin, P.-E., 2012, Optimization of the volume ablation rate for metals at different laser pulse-durations from ps to fs, 8243/:824307--13.

[10] Ronny Pfeifer ∗, D. H., Michael Hustedt, Stephan Barcikowski, 2010, Pulsed Nd:YAG laser cutting of NiTi shape memory alloys—Influence of process parameters.

[11] U. Engelhardt, J. H., K. Dickmann, 2012, Abtragsverhalten verschiedener Werkstoffe beim Mikrostrukturieren mit Pikosekundenlasern in Kombination mit einer Scanoptik.

[12] Yeo, C. Y., Tam, S. C., Jana, S., Lau, M. W. S., 1994, A technical review of the laser drilling of aerospace materials, Journal of Materials Processing Technology, 42/1:15-49.